Modelling of Mass Transfer in a Direct Methanol Fuel Cell

A DISSERTATION

Submitted in Partial Fulfillment of the Requirements for the Degree of

Master of Technology

In

CHEMICAL ENGINEERING

(Industrial Safety and Hazard Management)

by

Pushpender Rawat

Department of Chemical Engineering

Indian Institute of Technology

Roorkee-247667 (India)

June, 2013

CANDIDATE'S DECLARATION

I hereby assure that the work entitled **"MODELLING OF MASS TRANSFER IN A DIRECT METHANOL FUEL CELL"** being presented in this dissertation report for the partial fulfillment of the award of M.Tech (Master of Technology) in Chemical Engineering with specialization in Industrial Safety & Hazard Management is an authentic record of my own work carried out under the supervision of **Dr. Prakash Biswas**, Department of Chemical Engineering, Indian Institute of Technology Roorkee, Roorkee.

The matter presented in this report has not been submitted by me for the award of any other degree of this or any other institute.

Place: Roorkee **Pushpender Rawat**

Enroll. No: 11516009

Date:

CERTIFICATE

This is to certify that above statement made by the candidate is correct to the best of my knowledge.

Dr. Prakash Biswas

Assistant Professor,

Department of Chemical Engineering

Indian Institute of Technology, Roorkee

Roorkee-247667, India.

Acknowledgement

It is a pleasure to thank the many people who made this thesis possible. Firstly, I thank the **Almighty** for everything he has given me.

It is difficult to overstate my gratitude to my supervisor, **Dr. Praksh Biswas** With his enthusiasm, his inspiration, and his great efforts to explain things clearly and simply, he helped to make the work interesting. Throughout my thesis-writing period, he provided encouragement, sound advice, good teaching, and lots of good ideas. I would have been lost without him. I am and shall be ever grateful to him for all the kindness and affection he had bestowed on me.

I am very thankful to my various course instructors for providing me good knowledge of various subjects. I am indebted to my many student colleagues, especially **Aditya Kumar** for providing a stimulating and fun environment in which to learn and grow. I gratefully acknowledge IIT Roorkee for providing me an excellent academic environment and facilities to carry out research.

Lastly, and most importantly, I wish to thank my parents and my family, for supporting, teaching and loving me. To them I dedicate this thesis.

Pushpender Rawat

Table of Contents

List of figures

List of Tables

Abstract

In this dissertation work, a mathematical, one-dimensional, steady-state model accounting for mass transfer, along with the electrochemical reactions taking place in the direct methanol fuel cell (DMFC), is developed. The model is based on some assumptions. We are interested in mass transfer because poor mass transfer leads to significant fuel cell performance loss, therefore to understand the mass transfer phenomenon in the direct methanol fuel cell deeply we have done the modelling of mass transfer in a DMFC. Methanol concentration goes on decreasing as we move from anode flow channel to membrane. This is because diffusion takes place in diffusion layer while in catalyst layer concentration decreases due to consumption. In AF region there is no loss in methanol concentration we have assumed that the anode flow region is to be treated as continuous stirred tank reactor (CSTR).

The methanol concentration is supposed to be zero in the membrane region but in actual some methanol crosses the membrane region and reaches then cathode side where it reacts with oxygen in the cathode catalyst region. This phenomenon is known as methanol crossover.

The model input is the model governing equations and the model output is the methanol and water concentrations in the anode flow (AF), anode diffusion (AD) and in anode catalyst (AC) regions. The model determines the net water transfer coefficient (α), which is an important parameter to describe the water management through the membrane in the direct methanol fuel cell. It describes the behavior of the net water transfer coefficient (α) with the current density of the cell. The model is implemented rapidly and suitable for real-time system direct methanol fuel cell calculations.

1.1 Fuel cell

Fuel cell is a direct electrochemical energy conversion device. It directly converts energy from one form (chemical energy) into another form (electrical energy). Unlike a battery a fuel cell cannot be depleted. It will continue to generate electricity as long as fuel is supplied (Fig. 1.)

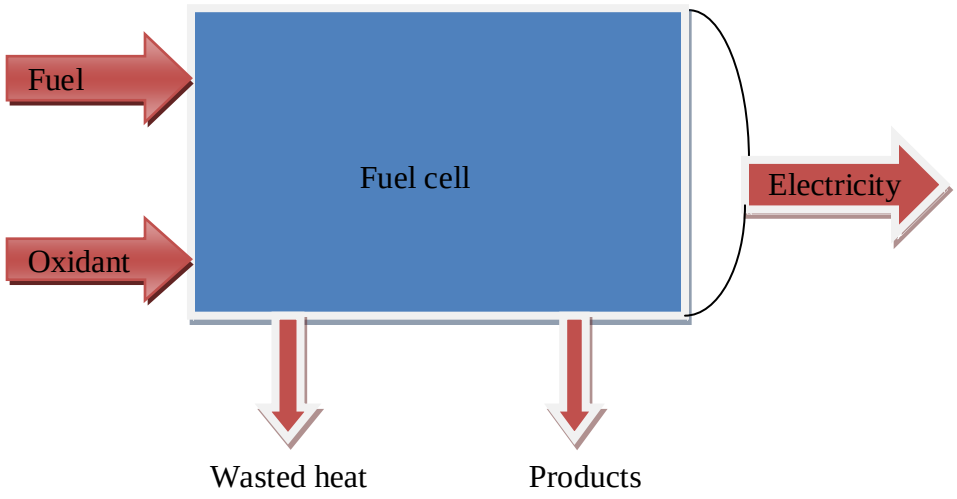

Fig.1. Schematic diagram of a fuel cell

1.2 Types of fuel cell

Fuel cells are classified based on electrolyte, chemical reactions taking place in the cell, the range of operating temperature, type of catalysts used and fuel required. The classification of different types of fuel cell is shown in the following table

Table 1

Classification of different types of fuel cell

Fuel cell type	Electrolyte	Charge carrier	Operating Temperature (^{o}C)	Fuel compatibility
(PEMFC)	Polymer membrane	H^+	$20-80^0$C	Hydrogen
Direct methanol fuel cell (DMFC)	Polymer membrane	H^+	$20-80^0$C	Methanol
(AFC)	Liquid KOH	OH^-	$60-220^0$C	Hydrogen
(PAFC)	Liquid H_3PO_4	H^+	200^0C	Hydrogen
(SOFC)	Ceramic	O^{2-}	$600-1000^0$C	Hydrogen, Methane and carbon monoxide
MCFC	Molten carbonate	CO_3^{2-}	650^0C	Hydrogen and Methane

1.2.1. Polymer Electrolyte Membrane Fuel Cell (PEMFC)

PEMFC uses a polymer membrane as an electrolyte. This polymer membrane is permeable to protons which are charge carriers in PEMFC. Hydrogen is used as a fuel and the pure oxygen is used as an oxidant. The hydrogen molecule breaks into protons and electrons at the anode. The hydrogen ions (protons) pass to the cathode through the electrolyte while the electrons produce electric power flowing through an external circuit Oxygen is supplied at the cathode and combines with the protons and the electrons to produce water.

1.2.2. Direct Methanol Fuel Cell (DMFC)

DMFC is similar to the PEMFC because the charge carrier is the hydrogen ion i.e. proton and the electrolyte is the polymer. As the DMFC withdraws the hydrogen from aqueous methanol so there is no need of a reformer. More details about DMFC is given later in this dissertation.

1.2.3. Alkaline Fuel Cell (AFC)

AFCs use an electrolyte which is an aqueous solution of (KOH) held in a porous stabilized matrix. The concentration of the solution can be varied with the operating temperature of the fuel cell which ranges from 65ºC to 220ºC.

The charge carrier for the AFCs is the hydroxyl ion (OH^-) which passes through the electrolyte from cathode to anode where it reacts with the hydrogen to generate electrons and water. Water formed at anode goes back to the cathode to regenerate hydroxyl ions (OH^-). The reactions in this type of fuel cell generate electricity and heat.

1.2.4. Phosphoric Acid Fuel Cell (PAFC)

The Phosphoric Acid Fuel Cells (PAFCs) use the phosphoric acid (which can approach high concentrations) as an electrolyte. The ionic conductivity of the phosphoric acid is low at low temperature, so the Phosphoric Acid Fuel Cells are operated at higher temperature ranges.

The charge carriers in this type of fuel cell are the hydrogen ions (protons). Similar to the PEMFC, the hydrogen produced at the anode is split into its electrons and protons. The protons move through the electrolyte and combine with oxygen, usually from air, at the cathode to form the water. The electrons are sent through an external circuit where they can perform the useful work. These reactions generate electricity and heat as by products.

1.2.5. Solid Oxide Fuel Cell (SOFC)

The Solid Oxide Fuel Cells (SOFCs) are the highest temperature fuel cells in development. To operate at the high temperature, the electrolyte is a thin, solid ceramic material (solid-oxide) which is conductive to the oxygen ions (O^{2-}), the charge carriers in the solid oxide fuel cell.

At cathode, oxygen molecules from air split into oxygen ions with the addition of four electrons. The oxygen ions are migrated through the electrolyte and combine with hydrogen at anode, releasing the four electrons. The electrons are routed through an external circuit generating electric power and heat.

1.2.6. *Molten Carbonate Fuel Cell (MCFC)*

MCFCs work rather differently from other fuel cells because they use the electrolyte which is composed of a molten mixture of carbonate salts. Two mixtures that can be used are potassium carbonate and lithium carbonate.

To melt the carbonate salt and to achieve the high ion mobility through electrolyte, the molten carbonate fuel cells operate at high temperature. On heating these salts melt and become conductive to the carbonate ions (CO_3^{2-}). These ions flow from cathode to the anode. At anode they combine with hydrogen to produce water, carbon dioxide and electrons. These electrons are routed through an external circuit back to the cathode, producing the electricity and heat.

1.3 Why DMFC – advantages and disadvantages

1.3.1. Advantages

- Methanol has much higher energy density than hydrogen stored in cylinders.
- Methanol is easier to handle and transport than pressurized hydrogen cylinders.
- Methanol is easy to refill.
- Being operated in an aqueous environment it has longer membrane life.
- There is no requirement for reactant humidification.
- DMFC system has quick start-up and load following
- DMFC system has lower weight and volume therefore it is simpler.

1.3.2 Disadvantages

- It operates at lower current density and lower cell voltage.
- DMFC fuel efficiency is lower (Approx. 17% at present).
- It requires a platinum catalyst to promote the power generation and platinum is an expensive metal.

1.4 Direct Methanol Fuel Cells (DMFC)

Direct Methanol Fuel Cell (DMFC) is the fuel cell in which aqueous methanol is used as a fuel. It contains two electrodes which are separated by a proton exchange membrane (PEM) and connected by an external circuit which allows the conversion of free energy into electrical energy from the chemical reaction of methanol with oxygen or air. DMFC operates at cold temperature, generating little heat with some machines operating around 70°C or 158°C.

Hydrogen fuel cells which operate on methanol use a separate reformer to release the hydrogen from the aqueous methanol and then the hydrogen is fed into the fuel cell

A schematic diagram of a DMFC is shown below in the figure.

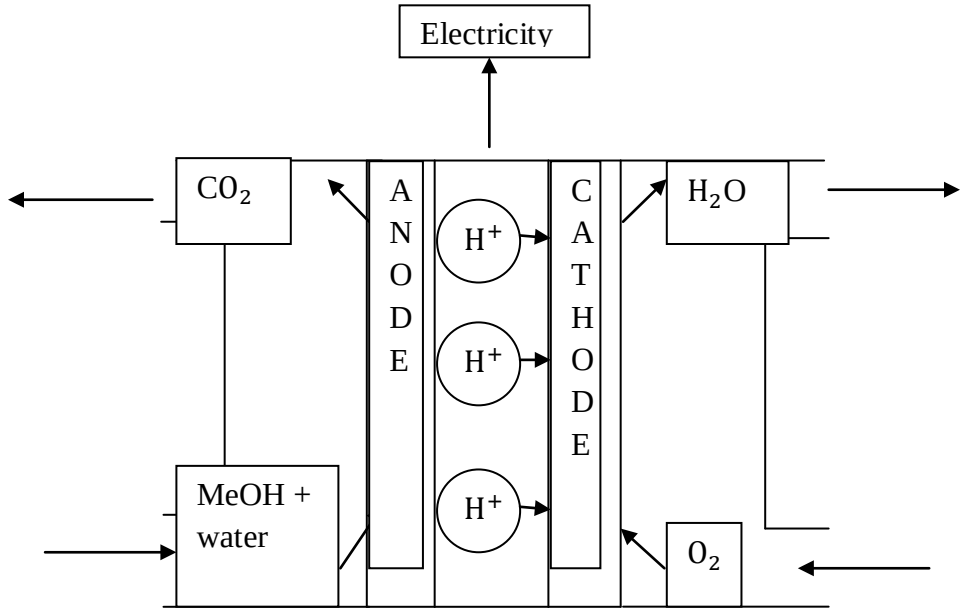

Fig. 2. Diagram of a direct methanol fuel cell.

1.5 Working Principle of DMFC

Basically, DMFC is a PEM fuel cell which is fed with a solution of methanol and water. The two catalytic electrodes anode (where the methanol oxidation takes place) and the cathode (where the oxygen reduction takes place) are separated by a membrane in which protons are conducted from anode to cathode. The combination of membranes and electrodes is called membrane electrode assembly (MEA). Each electrode is made of a gas diffusion layer (GDL) and a catalytic layer Fig. 3.

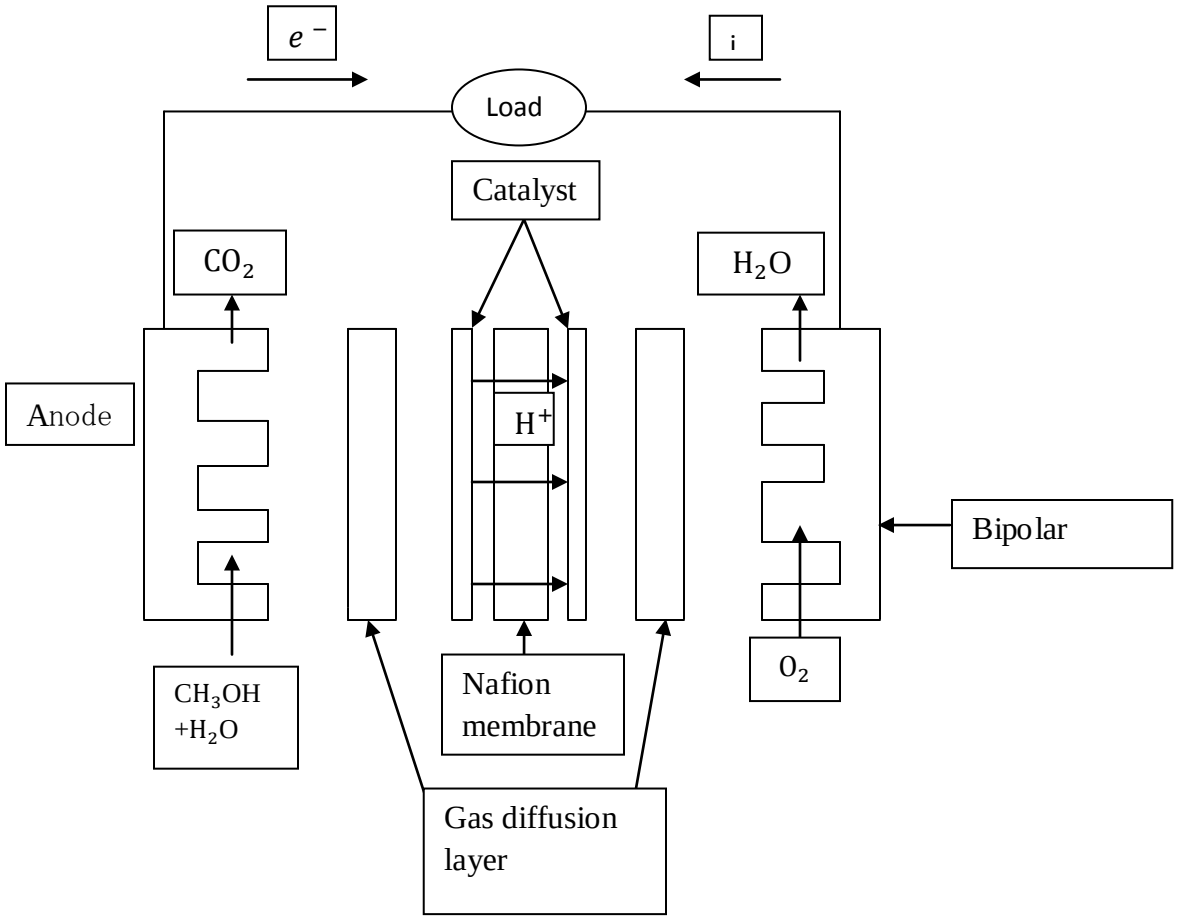

Fig. 3. working structure of a direct methanol fuel cell

Methanol and water solution is fed at the anode side which is diffused through the diffusion layer to the catalytic layer where it is oxidized into carbon dioxide, protons and electrons.

1.6 Mass Transfer and its Significance in DMFC

As discussed earlier, to produce electricity, a fuel cell must be continuously supplied with fuel and oxidant. At the same time products must be continuously removed to avoid "strangling" the cell. This process of supplying reactants and removing products is known as fuel cell mass transfer.

We are interested in mass transfer because poor mass transfer leads to significant fuel cell performance loss. To understand why poor mass transport can lead to a performance loss, we have to remember that fuel cell performance is determined by the reactant and product concentrations within the catalyst layers, not at the fuel cell inlet.

Methanol concentration goes on decreasing as we move from anode flow channel to membrane. This is because diffusion takes place in diffusion layer while in catalyst layer concentration decreases due to consumption. In AF region there is no loss in methanol concentration we have assumed that the anode flow region is to be treated as continuous stirred tank reactor (CSTR).

The methanol concentration is supposed to be zero in the membrane region but in actual some methanol crosses the membrane region and reaches then cathode side where it reacts with oxygen in the cathode catalyst region. This phenomenon is known as methanol crossover.

1.7 Methanol Crossover

Methanol crossover is an unwanted issue in the DMFC. As discussed earlier when methanol crosses the membrane it reacts with the oxygen at cathode side. This reaction creates short circuit which lowers the fuel cell efficiency. So for better efficiency methanol concentration should be minimum. It can be minimized by the following ways

- By using the low concentration of methanol
- By using the high current density

1.8 Applications of DMFC

DMFCs are one of the possible solutions to supply clean energy production in this time of limiting petroleum resources. As DMFCs can be stacked according to the demand to increase the energy output, these have wide ranges of uses.

1.8.1. Stationary power

DMFCs can potentially generate electricity for commercial, homes, institutions and for industries through stationary power plants. The range of electricity produced is from 1KW to several MW which is enough for industries and institutions. Small fuel cell power plants can be installed for residential applications for generation of electricity and heat.

1.8.2.Transportation power

An important commercial application of DMFCs is to replace the IC engine in transportation. Today, all the major automobile companies are trying to develop prototype fuel cell vehicles. There are many vehicles in the different stages of demonstration.

1.8.3.Portable power

DMFCs have the applications in the area of portable power viz. powering laptops, cellular phones, and palm pilots hours longer than batteries. Some major Companies have already demonstrated them for powering cell phones for 30 days without recharging and laptops for 20 hours. Other applications include pagers, portable power, and video recorders.

Hikita *et al.* [18] found out the methanol crossover rates by measuring the methanol concentration continuously. A common method to determine the methanol crossover in a direct methanol fuel cell is the analysis of carbon dioxide content in the cathode exhaust. However it is important to mention that during the operation of a direct methanol fuel cell, carbon dioxide is produced in a large amount at anode oxidation and a part of it can diffuse partially at cathode side. In that case the amount of carbon dioxide present in the exhaust is a reason of the carbon dioxide coming from methanol crossover oxidation at the cathode side.

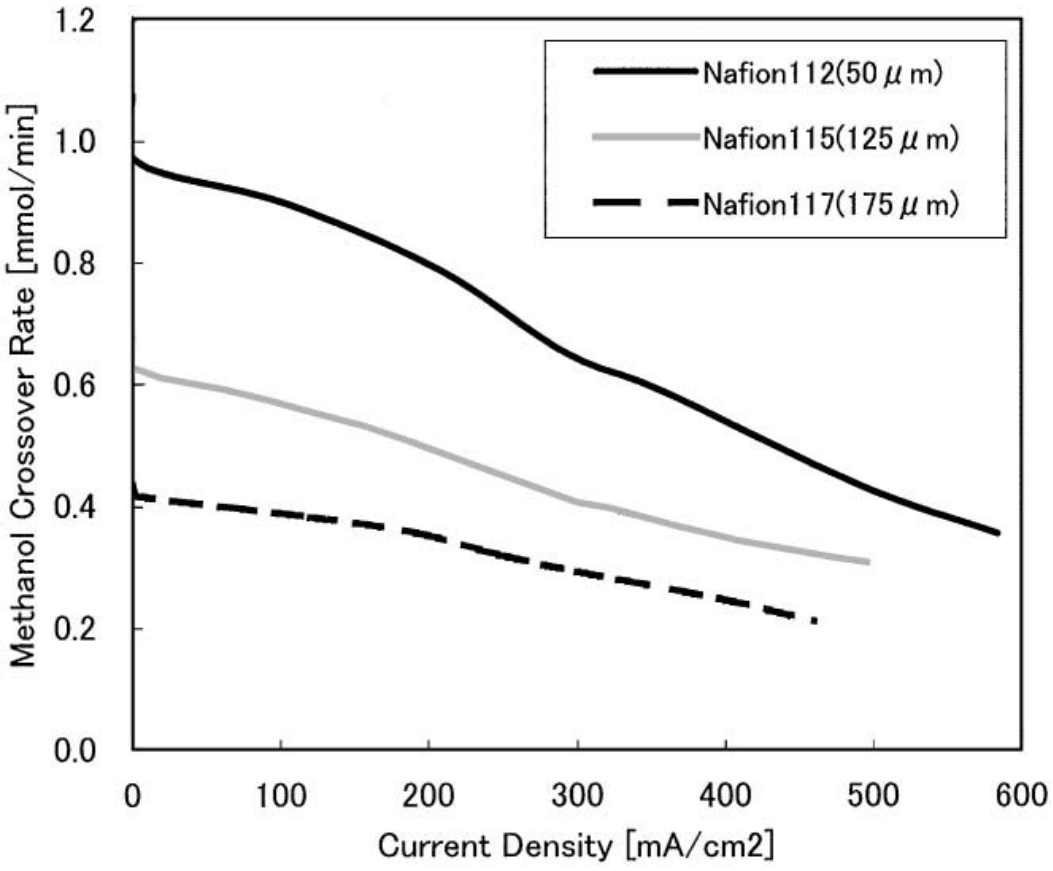

Fig. 4. Influence of the membrane thickness on methanol crossover Rate [18]

In the above work Dohle *et al.* [24] reported a method to differentiate the two reasons under real direct methanol fuel cell operating conditions and clearly determine the amount of carbon dioxide resulting from methanol crossover at cathode side.

Ramya and Dhathathreyan [35] measured the methanol flux rates across the Nafion membrane straight away by an electrochemical method, like chronoamperometry. This technique measured the membrane permeability for different methanol concentrations. They found that the methanol permeability is dependent on the methanol concentration, permeability increases with the increase in the methanol concentration. The need of calculating methanol crossover by a faster and a simple method than conventional method of carbon analysis has become significant.

Munichandraiah *et al.* [37] has reported a potentiometric method. According to it, the slope (dE/dt) of the curve E_{cell} versus (t) is directly proportional to the methanol crossover rate. Methanol crossover rate has been evaluated by the time required to reach the methanol concentration (equilibrium) at both side of the membrane.

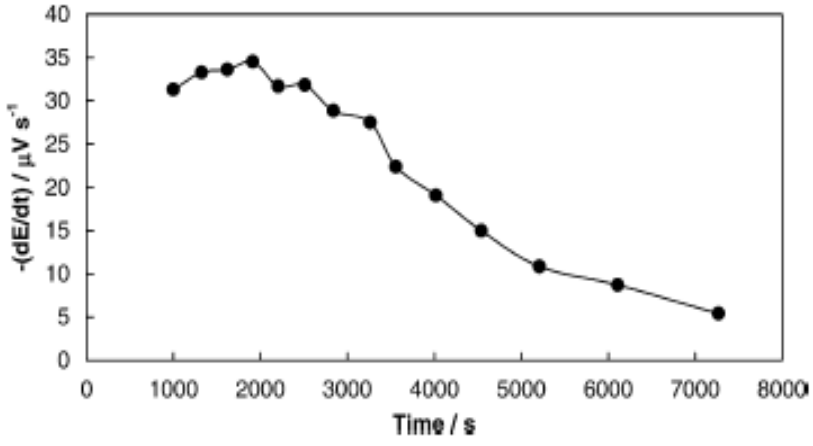

Fig. 5. variation of (dE/dt) during methanol crossover [37]

Jiang and Chu [56] approximated the amount of the methanol crossover with more accuracy by a method of gravimetric determination of barium carbonate to examine the amount of carbon dioxide. The equivalent methanol crossover current was calculated from the sum of dry barium carbonate precipitate at anode and cathode exhaust and the discharge current of the fuel cell. With the help of this method the experimental deviation for measuring the methanol crossover by carbon dioxide permeation through PEM can be corrected.

Park *et al.* [39] represented a practical method of characterizing mass transfer phenomenon in membrane electrode assemblies through mass balance research in direct methanol fuel cell systems. This method could be used to determine methanol utilization efficiency, net water transport coefficient and the conversion rate of methanol to electricity of a membrane electrode assembly in DMFCs.

The research on DMFC was performed to minimize the methanol and water crossover keeping high power characteristics. By changing the material properties, the critical design parameters were described for high methanol utilization.

The effects of methanol crossover on the DMFC performance have been studied in the literature under operating conditions, such as, cathode air pressure, methanol concentration, temperature, membrane thickness, fuel flow rate and catalyst morphology.

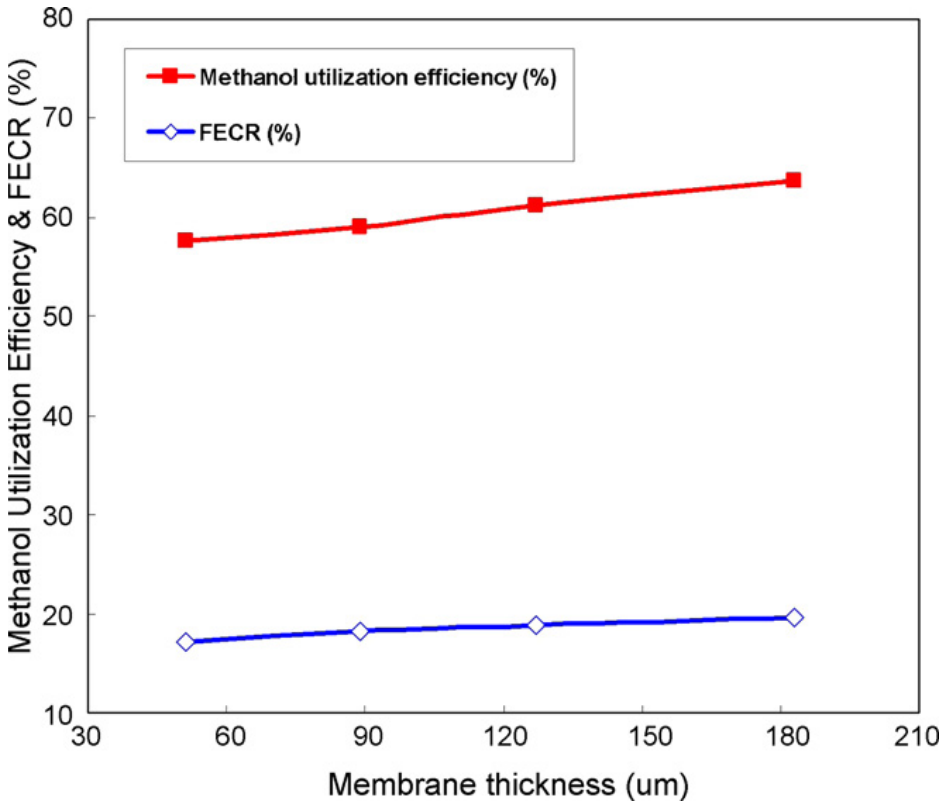

Fig. 6. The methanol utilization efficiency and the FECR as a function of membrane thickness [39]

Gogel *et al.* [42] represented the investigations to evaluate the dependence of the performance of the DMFC and the methanol crossover rate on operating conditions, on the noble metal loading and on the structure of the electrodes. It was observed that the performance and the methanol permeation strongly depend on cathode air flow and cell temperature.

Also, methanol permeation can be minimized significantly by changing the anode structure, but the changed structure also causes of marginally lower power densities. At anode and cathode the metal loading was varied, affecting the cell performance. Further the differences between unsupported and supported catalysts were compared. They also described the optimum conditions for the DMFC operation taking in consideration the various important factors.

Du *et al.* [55] developed a half cell containing a normal DMFC cathode and a membrane consisting of an electrolyte solution to observe the effect of methanol crossover. Cyclic volummetry profiles, open circuit potentials, chemical science electrical resistance, spectroscopic analysis and polarization curves, resulting from oxygen reduction with or without the effect of methanol oxidation were measured.

The steady state results verified that the methanol presence at cathode side led to a significant poisoning effect on oxygen reduction particularly when direct methanol fuel cell discharge at lower potentials and operate at higher methanol concentrations.

A mathematical model has been developed based on some assumptions to deeply understand the mass transfer phenomenon in a direct methanol fuel cell.

3.1 model structure

The schematic diagram of a direct methanol fuel cell consisting of all layers is shown in the Fig. 4.

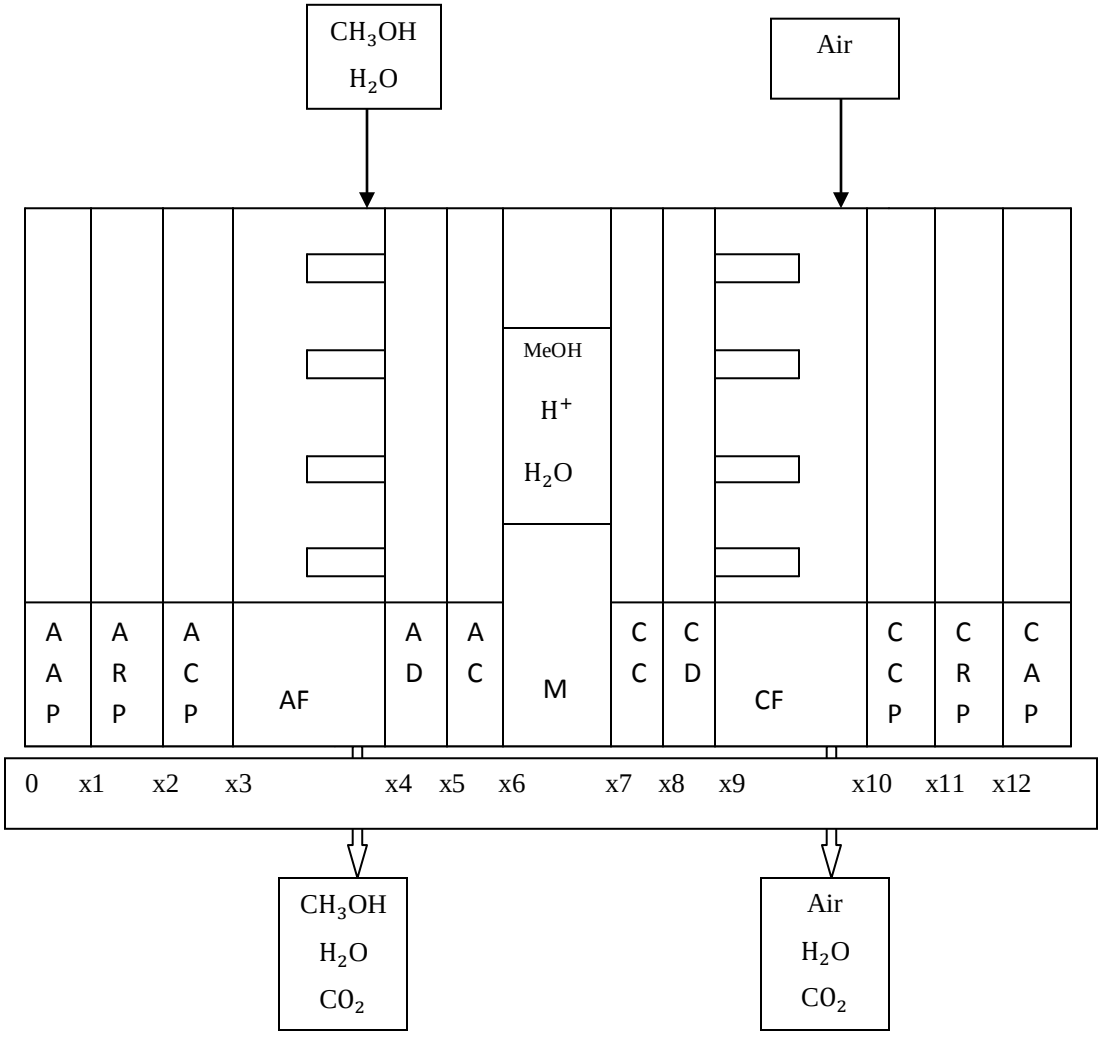

Fig. 7. Model structure of a direct methanol fuel cell.

A DMFC consists of the following parts

A copper plate (CP), a rubber plate (RP) and an aluminum plate (AP) at both anode and cathode side. At anode side these plates are known as (ACP), (ARP) and (AAP) while at cathode side they are known as (CCP), (CRP) and (CAP).

A flow channel (F), a diffusion layer (D) and a catalyst layer (C) at both anode and cathode side. At anode side these are termed as (AF), (AD) and (AC) while at cathode side these are known as (CF), (CD) and (CC).

An aqueous solution of methanol is supplied in the anode flow channel with the help of a liquid pump and air is supplied to cathode side with the help of a mass flow controller. From diffusion layer to catalyst layer and from catalyst layer to the membrane the transfer of methanol is due to the diffusion.

Reactions take place in the catalyst layers. In AC, reaction of methanol oxidation takes place with the releasing of carbon dioxide while in CC oxygen reacts with electrons and protons to generate water.

3.2 Assumptions

DMFC is a multiphase system which involves coincident mass, charge and energy transfer. To make this system simpler it is here described as a one-dimensional transport (along the x direction) with the following and assumptions:

- It is assumed to operate under steady-state condition.
- Mass transfer in diffusion layer and the membrane is described using Fick's model.
- Mass transfer in gas diffusion layer (GDL) and in catalyst layer is assumed to be a diffusion-predominated process
- Effect of the convection is neglected.
- Pressure gradient is neglected across the layers.
- At anode side only liquid phase is considered therefore carbon dioxide remains dissolved in the solution.
- At cathode side gaseous methanol and water are considered.
- Solutions are assumed to be idle and dilute.
- Partition functions represent local equilibrium at interfaces.
- Water and methanol transfer through membrane is assumed due the combined effect of conc. gradient between cathode and anode and electro-osmosis force.
- The anode and the cathode flow channels are considered as CSTR. Therefore composition inside these flow channels is uniform.

3.3 Governing equations and Boundary conditions

Anode side

Methanol oxidation: $CH_3OH + H_2O \rightarrow CO_2 + 6H^+ + 6e^-$ (1)

Cathode side

Oxygen reduction: $\frac{3}{2} O_2 + 6H^+ + 6e^- \rightarrow 3H_2O$ (2)

Overall reaction: $CH_3OH + \frac{3}{2} O_2 \rightarrow 2H_2O$ (3)

The anode flow channels are considered as a continuous stirred tank reactor (CSTR), so the water and methanol fluxes are given by

$$N_j = \frac{q^{AF}}{A^S}(C_{j-}^0 C_j^{AF}) \quad (4)$$

Where *j* represents water or methanol

$$A^s = \eta_{\text{channels}} \times e \times w \quad (5)$$

where η_{channels} is the channel number and w and e are the length and width of the channels, respectively.

In the anode diffusion layer and catalyst layer, the water and methanol flux are related to the concentration gradient with an effective diffusivity -$D_j^{eff,AD}$ in the AD and -$D_j^{eff,AC}$ in the AC. The methanol and water flux can be obtained from:

$$N_j = -D_j^{eff,AD} \frac{dC_j^{AD}}{dx} \quad (6)$$

and

$$N_j = -D_j^{eff,AC} \frac{dC_j^{AC}}{dx} \quad (7)$$

Where *j* represents water or methanol

The concentration at the AF/AD and AD/AC interfaces is determined by assuming local equilibrium with a partition coefficient K_4 and K_5, respectively. The B.C. for Eq. (6) and (7) are

At x = x_4 ; $C_j^{AD} = K_4 C_j^{AF}$ (8)

At x = x_5 ; $C_j^{AC} = K_5 C_j^{AD}$ (9)

At x = x_6 ; $C_j^{AC} = K_6 C_j^{AC}$ (10)

In DMFC, the methanol flux is related to the current density and the permeation flux of methanol through the membrane, ($N_{CH_3OH}^M$) by

$$N_{CH_3OH} = \frac{I_{cell}}{6F} + N_{CH_3OH}^M \quad (11)$$

Water flux is related with the current density and to the net water transport coefficient(α) at anode side by:

$$N_{H_2O} = \frac{I_{cell}}{6F}(1+\alpha) \quad (12)$$

The mass transfer of methanol and water through the membrane is assumed to be due to the combined effect of the concentration gradient and the electro-osmosis force. The fluxes can be obtained from:

$$N^{M}_{CH_3OH} = -D^{eff,M}_{CH_3OH}\frac{dC^{M}_{CH_3OH}}{dx} + \xi_{CH_3OH}\frac{I_{cell}}{F} \quad (13)$$

$$N^{M}_{H_2O} = -D^{eff,M}_{H_2O}\frac{dC^{M}_{H_2O}}{dx} + \eta_d\frac{I_{cell}}{F} = \alpha\frac{I_{cell}}{6F} \quad (14)$$

The net water transport coefficient, (α), can be determined by solving the equation (14).

The concentration at the AC/membrane interface is given by assuming the local equilibrium with a partition coefficient K_6. The boundary conditions for the integration of equations (13) and (14) is given by

At $x = x_6$; $C^{M}_{j} = K_6 C^{AC}_{6,j}$ (15)

Where *j* represents water or methanol

In the cathode catalyst region, the water, oxygen and methanol flux are related to the concentration gradient with an effective diffusivity -$D^{eff,CC}_{j}$ The flux can be obtained from:

$$N_j = -D_j^{eff,CC} \frac{dC_j^{CC}}{dx} \quad (16)$$

Here it is assumed that the whole methanol crossing the membrane reacts in the cathode catalyst region therefore the concentration at the CC/CD interface is zero**.** It is also considered that there is no oxygen crossover, therefore the oxygen concentration in CC/M interface is zero. The concentration of water and methanol at the membrane/CC interface and the concentration of water and oxygen at the CC/CD interface are given by assuming local equilibrium with a partition coefficient K_7 and K_8, respectively. The boundary conditions for equation (16) are:

At $x = x_7$; $C_j^{CC} = C_{7,j}^{CC} = K_7 C_{7,j}^{M}$, j represents methanol or water and $C_{7,O_2}^{cc} = 0$ (17)

At $x = x_8$; $c_{CH_3OH}^{cc} \cong 0$, $c_{H_2O}^{cc} = c_{8,H_2O}^{cc}$ and $c_{O_2}^{cc} = c_{8,O_2}^{cc}$ (18)

In the the cathode catalyst layer, oxygen reacts with the protons and electrons to generate water. However some part of oxygen fed is consumed due to methanol crossover to form an internal current. So the oxygen flux is related to the current density of the fuel cell and the permeation flux of methanol through the membrane by

$$N_{o_2} = \upsilon o_2 \frac{I_{cell}}{4F} + \upsilon_{cross,} o_2 N_{CH_3OH}^{M} \quad (19)$$

Where $\upsilon o_2 = 1$ and $\upsilon_{cross,} o_2 = 3/2$

At the cathode side, the water flux is related with the water produced from the oxygen reduction reaction, methanol crossover oxidation and to the net water flux transferred from the anode to the cathode by:

$$N_{H_2O} = \upsilon_{H_2O} \frac{I_{cell}}{4F} + \upsilon cross,_{H_2O} N^{M}_{CH_3OH} + N^{M}_{H_2O} \quad (20)$$

In the cathode diffusion layer the oxygen and water flux are related to the concentration gradient by

$$N_i = -D_i^{eff,CD} \frac{dC_i^{CD}}{dx}, \ i \text{ represents oxygen or water vapor} \quad (21)$$

Where $D_i^{eff,CD}$ is the effective diffusion coefficient of oxygen and water in the CD.

The concentration at the CF/CD and CD/CC interfaces is given by considering local equilibrium with a partition coefficient K_9 and K_8. The boundary conditions for Eq. (21) are

At x = x_8 ; $C_i^{CD} = K_{8,i} C_{8,i}^{CC}$ (22)

At x = x_9 ; $C_i^{CF} = K_{9,i} C_i^{CD}$ (23)

Like at the anode side, the cathode flow channels are also treated as a continuous stirred tank reactor
(CSTR), so the oxygen and water vapor flux are described by

$$N_i = \frac{q^{CF}}{A^S} (C_{i-}^0 C_i^{CF}) \quad (24)$$

where *i* represents water or oxygen vapor and

$$A^s = \eta_{channels} \times e \times w \tag{25}$$

At cathode if dry air is fed, the water vapor feed concentration ($c^0_{H_2O}$) is zero.

To understand the effect of methanol crossover on the cathode over potential it is considered that the methanol crossing the membrane completely reacts electrochemically at the cathode. So the internal current (I_{CH_3OH}) due to methanol oxidation will be

$$I_{CH_3OH} = 6F\, N^{M}_{CH_3OH} \tag{26}$$

3.4 Solutions

The water and methanol concentration profile in AF can be get by combining Equations (4) and (12) or (4) and (11):

$$C_{CH_3OH}^{AF} = C_{CH_3OH}^{0} - \frac{A^S}{q^{AF}}\left(\frac{I_{cell}}{6F} + N_{CH_3OH}^{M}\right) \quad (27)$$

$$C_{H_2O}^{AF} = C_{H_2O}^{0,AF} - \frac{A^S}{q^{AF}}\frac{I_{cell}}{6F}(\alpha + 1) \quad (28)$$

Combining equations (6), (8) and (11) or (12) gives the concentration profile in AD. To get the concentration profile in AC we combine Equations (7), (9) and (11) or (12). The solutions are

$$C_{CH_3OH}^{AD} = K_4 C_{CH_3OH}^{AF} + \frac{I_{cell}}{6FD_{CH_3OH}^{eff,AD}}(x_4\text{-x}) + \frac{N_{CH_3OH}^{M}}{D_{CH_3OH}^{eff,AD}}(x_4\text{-x}) \quad (29)$$

$$C_{H_2O}^{AD} = K_4 C_{H_2O}^{AF} + \frac{I_{cell}\,(\alpha+1)}{6FD_{H_2O}^{eff,AD}}(x_4\text{-x}) \quad (30)$$

$$C_{CH_3OH}^{AC} = K_5 C_{CH_3OH}^{AD} + \frac{I_{cell}}{6FD_{CH_3OH}^{eff,AC}}(x_5\text{-x}) + \frac{N_{CH_3OH}^{M}}{D_{CH_3OH}^{eff,AC}}(x_5\text{-x}) \quad (31)$$

$$C_{H_2O}^{AC} = C_{5,H_2O}^{AC} + \frac{I_{cell}\,(\alpha+1)}{6FD_{H_2O}^{eff,AC}}(x_5\text{-x}) \quad (32)$$

The concentration of methanol and water through the membrane can be obtained by using Equations (13) and (14):

$$C^{M}_{\mathrm{CH_3OH}} = K_6 C^{AC}_{CH_3\mathrm{OH}} + \frac{\mathrm{N}^{\mathrm{M}}_{CH_3\mathrm{OH}} - \frac{\xi_{CH_3\mathrm{OH}}\ \mathrm{I_{cell}}}{\mathrm{F}}}{D^{eff,M}_{\mathrm{CH_3OH}}}(x_6\text{-x}) \quad (33)$$

$$C^{M}_{H_2\mathrm{O}} = K_6 C^{AC}_{H_2\mathrm{O}} + \frac{\alpha\ \mathrm{I_{cell}}}{6\mathrm{F}D^{eff,M}_{H_2\mathrm{O}}}(x_6\text{-x}) - \frac{\eta_d \mathrm{I_{cell}}}{\mathrm{F}D^{eff,M}_{H_2\mathrm{O}}}(x_6\text{-x}) \quad (34)$$

Combining equations. (13), (15) and (17) we obtained an expression to calculate the methanol flux through the membrane:

$$\mathrm{N}^{\mathrm{M}}_{CH_3\mathrm{OH}} = \frac{D^{eff,M}_{CH_3\mathrm{OH}}}{\delta^M}(K_6 C^{AC}_{6,CH_3\mathrm{OH}} - C^{M}_{7,CH_3\mathrm{OH}}) + \frac{\xi_{CH_3\mathrm{OH}}\ \mathrm{I_{cell}}}{\mathrm{F}} \quad (35)$$

The concentration of methanol, water and oxygen through the CC can be obtained combining Equations (16), (17) and (18):

$$C^{CC}_{\mathrm{CH_3OH}} = C^{CC}_{7,CH_3\mathrm{OH}} - \frac{\mathrm{I_{cell}}}{6\mathrm{F}D^{eff,CC}_{CH_3\mathrm{OH}}}(x_7\text{-x}) + \frac{\mathrm{N}^{\mathrm{M}}_{CH_3\mathrm{OH}}}{D^{eff,CC}_{\mathrm{CH_3OH}}}(x_7\text{-x}) \quad (36)$$

$$C^{CC}_{H_2\mathrm{O}} = C^{CC}_{7,H_2\mathrm{O}} + \frac{(x_7-\mathrm{x})}{D^{eff,CC}_{H_2\mathrm{O}}}\left(\frac{\alpha \mathrm{I_{cell}}}{6F} + \frac{.5\mathrm{I_{cell}}}{F} + \frac{\mathrm{I}_{CH_3\mathrm{OH}}}{3F}\right) \quad (37)$$

$$C^{CC}_{O_2} = C^{CC}_{8,O_2} + \frac{\mathrm{I_{cell}}}{6\mathrm{F}D^{eff,CC}_{O_2}}(x_8\text{-x}) + \frac{3\mathrm{N}^{\mathrm{M}}_{CH_3\mathrm{OH}}}{2\ D^{eff,CC}_{O_2}}(x_8\text{-x}) \quad (38)$$

Combining equations (19), (21) and (22) or (20), (21), and (22) we obtained the concentration profile in CD:

$$C_{O_2}^{CD} = K_{8,O_2} C_{8,O_2}^{CC} + \frac{\mathrm{I_{cell}}}{6\mathrm{F}D_{O_2}^{eff,CD}}(x_8\text{-x}) + \frac{3\mathrm{N}_{CH_3OH}^{M}}{2\,D_{O_2}^{eff,CD}}(x_8\text{-x}) \quad (39)$$

$$C_{H_2O}^{CD} = K_{8,H_2O} C_{8,H_2O}^{CC} + \frac{(x_8-\mathrm{x})}{D_{H_2O}^{eff,CD}}\left(\frac{\alpha \mathrm{I_{cell}}}{6F} + \frac{.5\mathrm{I_{cell}}}{F} + \frac{\mathrm{I}_{CH_3OH}}{3F}\right) \quad (40)$$

The concentration of oxygen and water through the CF can be obtained using Equations (19) and (24) or (20) and (24):

$$C_{O_2}^{CF} = C_{O_2}^{0} - \frac{A^S}{q^{CF}}\left(\frac{\mathrm{I_{cell}}}{6F} + \frac{3\mathrm{N}_{CH_3OH}^{M}}{2}\right) \quad (41)$$

$$C_{H_2O}^{CF} = C_{H_2O}^{0,CF} + \frac{A^S}{q^{CF}}\left(\frac{\alpha \mathrm{I_{cell}}}{6F} + \frac{.5\mathrm{I_{cell}}}{F} + \frac{\mathrm{I}_{CH_3OH}}{3F}\right) \quad (42)$$

From the solutions above we get an expression to calculate the C_{6,CH_3OH}^{AC}, C_{7,CH_3OH}^{M}, C_{8,O_2}^{CC} and α

$$C_{6,CH_3OH}^{AC} = (K_5K_4C_{CH_3OH}^0 - \frac{I_{cell}}{6F} C_1 - \frac{\xi_{CH_3OH} I_{cell}}{F} C_1 + \frac{D_{CH_3OH}^{eff,M} C_{7,CH_3OH}^M}{\delta^M} C_1)/(1 + \frac{D_{CH_3OH}^{eff,M}}{\delta^M} K_6C_1) \quad (43)$$

Where

$$C_1 = \frac{\delta^M}{D_{CH_3OH}^{eff,AD}} K_5 + \frac{\delta^{AC}}{D_{CH_3OH}^{eff,AD}} - \frac{A^S}{q^{AF}} K_4 K_5 \quad (44)$$

$$C_{7,CH_3OH}^M = (- \frac{I_{cell} \delta^{CC}}{6FD_{CH_3OH}^{eff,CC} K_7} + \frac{\xi_{CH_3OH}\delta^{CC} I_{cell}}{FD_{CH_3OH}^{eff,CC} K_7} + \frac{D_{CH_3OH}^{eff,CC}\delta^{CC} K_6C_{6,CH_3OH}^{AC}}{\delta^M D_{CH_3OH}^{eff,CC} K_7})/(1 + \frac{D_{CH_3OH}^{eff,M} \delta^{CC}}{\delta^M D_{CH_3OH}^{eff,CC} K_7}) \quad (45)$$

$$C_{6,H_2O}^M = K_4K_5K_6C_{H_2O}^0 - \frac{C_3 I_{cell}}{6F} (1 + \alpha) \quad (46)$$

$$C_3 = \frac{\delta^{AC}}{D_{H_2O}^{eff,AD}} K_5 + \frac{\delta^{AD} K_5 K_6}{D_{H_2O}^{eff,AD}} + \frac{A^S}{q^{AF}} K_4 K_5 K_6 \quad (47)$$

$$C_{7,H_2O}^M = \frac{C_{H_2O}^0}{K_{7,H_2O}K_{8,H_2O}K_{9,H_2O}} + \left(\frac{\alpha I_{cell}}{6F} + \frac{I_{cell}}{2F} + \frac{I_{CH_3OH}}{3F} \right) C_4 \quad (48)$$

$$C_4 = \frac{\delta^{CD}}{K_{7,H_2O}K_{8,H_2O} D_{H_2O}^{eff,CD}} + \frac{\delta^{CC}}{K_{7,H_2O} D_{CH_3OH}^{eff,CC}} + \frac{A^S}{q^{AF}K_{7,H_2O}K_{8,H_2O}K_{9,H_2O}} \quad (49)$$

$$\alpha = \frac{-6FD_{H_2O}^{eff,M}}{I_{cell}} (\frac{C_{7,H_2O}^M - C_{6,H_2O}^M}{\delta^M}) + 6\eta_d \quad (50$$

Now to calculate methanol conc. in AF, AD, AC region we need the value of $N^{M}_{CH_3OH}$ which can be calculate from equation (35). For that we need to solve the equations (43) and (45) to get the values of C^{AC}_{6,CH_3OH} and C^{M}_{7,H_2O} respectively. Here we are using the following values of different parameters.

Table 2 (Temperature = 343K, Pressure = 1 atm.)

Parameter	Value	Reference
$D^{eff,AD}_{CH_3OH}$	4.827E-03 (cm^2/s)	31
$D^{eff,AC}_{CH_3OH}$	4.015E-03 (cm^2/s)	31
$D^{eff,CC}_{CH_3OH}$	3.165E-07 (cm^2/s)	31
$D^{eff,M}_{CH_3OH}$	6.0648E-06 (cm^2/s)	30
ξ_{CH_3OH}	7.5	32

From equation (44)

$$C_1 = -45.42648$$

And

$$C^{AC}_{6,CH_3OH} = (3.165139E\text{-}03 + 1.56607E\text{-}04\ I_{cell}) \quad (51)$$

$$N^{M}_{CH_3OH} = (4.26220245E\text{-}10 + 1.758756E\text{-}06\ I_{cell}) \quad (52)$$

$C_{CH_3OH}^{AF}$ = (4.99677E-04 – 2.6408E-04 I_{cell}) (53)

$C_{CH_3OH}^{AD}$ = (3.999742E-04 – 2.11264E-04 I_{cell}) + (8.828274E-08 +7.2202649E-04I_{cell}) (x_4-x)

(54)

$C_{CH_3OH}^{AC} = K_5 C_{CH_3OH}^{AD}$ + (1.06156973E-07 + 8.67998273E-04I_{cell}) (x_5-x) (55)

Now when we use the Table 3 parameters.

Table 3. (Temperature = 298K, Pressure = 1 atm.)

Parameter	value	Reference
$D_{CH_3OH}^{eff,AD}$	1.38E-05 (cm^2/s)	57
$D_{CH_3OH}^{eff,AC}$	5.2E-06 (cm^2/s)	57
$D_{CH_3OH}^{eff,CC}$	2.42E-07 (cm^2/s)	31
$D_{CH_3OH}^{eff,M}$	1.89E-06 (cm^2/s)	30
ξ_{CH_3OH}	1.99	Reference value

C_{6,CH_3OH}^{AC} = (3.19967E-04 - 3.9647E-01 I_{cell}) (56)

C_{7,CH_3OH}^{M} = (2.556638E-04 – 1.707688E-01 I_{cell}) (57)

$$N^{M}_{CH_3OH} = 3.2613E\text{-}11 + 1.7085E\text{-}06\ I_{cell} \quad (58)$$

$$C^{AF}_{CH_3OH} = 4.999985E\text{-}04 - 8.6232E\text{-}04\ I_{cell} \quad (59)$$

$$C^{AD}_{CH_3OH} = 3.999828E\text{-}04 - 1.14976E\text{-}03\ I_{cell} + (2.3626 + 2.488956E\text{-}01 I_{cell})\ (x_4\text{-}x) \quad (60)$$

Now to know the behavior of net water transport coefficient α with respect to current density we need to solve the equation (50). Which is

$$\alpha = \frac{-6F D^{eff,M}_{H_2O}}{I_{cell}} \left(\frac{C^{M}_{7,H_2O} - C^{M}_{6,H_2O}}{\delta^{M}}\right) + 6\eta_d$$

for this equation to be solved first we have to solve the equations (46) and(48) to get the values of C^{M}_{6,H_2O} and C^{M}_{7,H_2O} respectively.

$$C^{M}_{6,H_2O} = 4.5568E\text{-}03 - I_{cell}.6.9371E\text{-}05\ (\alpha + 1) \quad (61)$$

$$C^{M}_{7,H_2O} = 1.390625E{+}01 + \alpha.\ I_{cell}\ 82.1422 + 2.4642833E{+}02 I_{cell} \quad (62)$$

By putting the equations (61) and (62) in equation (50) we can obtain the value of α

$$\alpha = -\left(\frac{.169165}{I_{cell}} + 2.9971\right) \quad (63)$$

negative sign shows that flow is in opposite direction.

Now to obtain water concentration in AF,AD,AC,M region we have to solve the equations (28), (30),(32) and (34) by putting the value of α.

$$C_{H_2O}^{AF} = 5.9E\text{-}02 - 5.22729E\text{-}04I_{cell} \quad (64)$$

$$C_{H_2O}^{AD} = (4.72E\text{-}02 - 4.18183E\text{-}04I_{cell}) + (3.08993E\text{-}05 + 7.30102E\text{-}04I_{cell})(x_4 - x) \quad 65)$$

$$C_{H_2O}^{AC} = K_5 C_{H_2O}^{AD} + (4.1551263E\text{-}05 + 9.8179028E\text{-}04I_{cell})(x_5 - x) \quad (66)$$

$$C_{H_2O}^{M} = (K_6 C_{H_2O}^{AC} - 5.279871E+05I_{cell})(x_6 - x) \quad (67)$$

Model equation (53) is solved for methanol concentration in anode flow region. This equation is independent of the thickness of the anode flow region and dependent to the current density only. So we varied the values of current density from 0.05 to 0.15 A/cm^2 in equation (53) to get the methanol concentration at different current densities. The methanol concentration for different values of current densities is shown in the Table 4.

Table 4

Methanol concentration for different current density in anode flow region (operating conditions temperature = 343K, pressure = 1 atm.)

Current density (A/cm^2)	Methanol concentration (M)
0.05	4.86764E-04
0.1	4.7356E-04
0.15	4.60356E-04

As it has been discussed above that the methanol concentration in anode flow region is independent of the thickness (x) of the layer, therefore the graph of methanol concentration with respect to thickness (x) will be constant as shown in the Fig. 8.

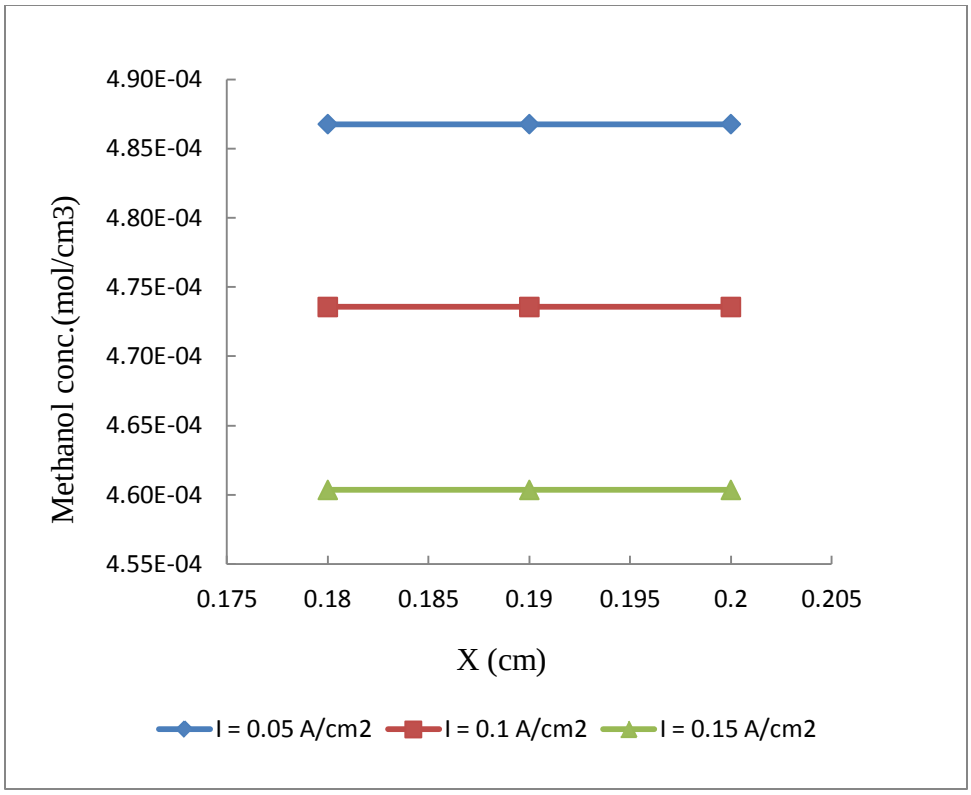

Fig. 8. Methanol concentration profiles in anode flow region (operating conditions: temperature = 343K, pressure = 1 atm.).

Methanol concentration is constant in the anode flow region because we have assumed that the anode flow region will be treated as a CSTR. For low current density methanol concentration is high while foe higher current density methanol concentration is lower.

Similarly model equation (54) is solved for methanol concentration in anode diffusion region is This equation is dependent on both thickness of the anode diffusion region and the current

density. So we varied the values of the thickness from 0.2 cm to 0.215 cm and current density from 0.05 to 0.15 A/cm^2 in equation (54) to get the methanol concentration at different current densities. The methanol concentration for different values of current densities is shown in the following Table 5.

Table 5

Methanol concentration for different current density in anode diffusion region (operating conditions: temperature = 343K, pressure = 1 atm.)

Thickness (x) cm	Methanol concentration (M) for I_{cell} = 0.05 A/cm^2	Methanol concentration (M) for I_{cell} = 0.1 A/cm^2	Methanol concentration (M) for I_{cell} = 0.15 A/cm^2
0.2	3.89411E-04	3.78848E-04	3.68285E-04
0.205	3.8923E-04	3.78486E-04	3.67743E-04
0.21	3.89049E-04	3.78125E-04	3.67201E-04
0.215	3.88868E-04	3.77763E-04	3.66659E-04

In anode diffusion region methanol concentration decreases with respect to the value of thickness (x) and this decreasing rate is minimum for low current density and maximum for higher current density. This is because diffusion takes place in the anode diffusion layer which decreases the methanol concentration.

The methanol concentration in anode diffusion region is shown in the Fig. 9.

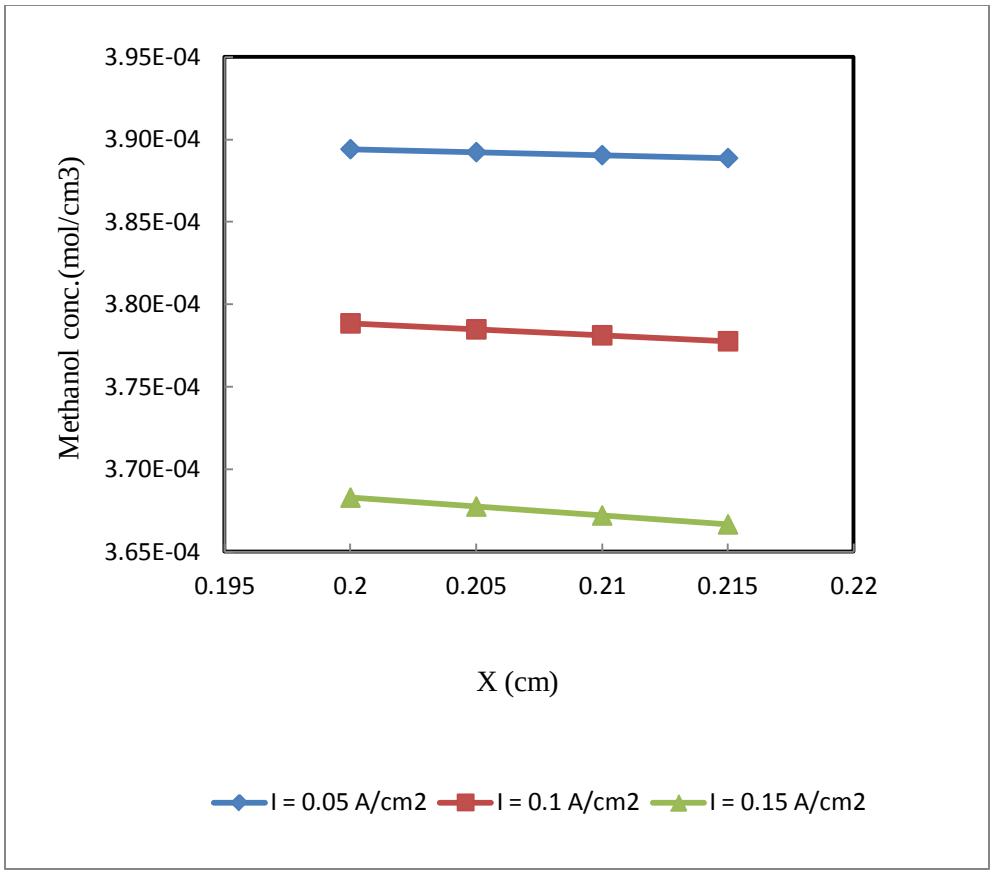

Fig. 9. Methanol concentration profiles in anode diffusion region (operating conditions: temperature = 343K, pressure = 1 atm.).

Similarly model equation (55) is solved for methanol concentration in anode catalyst region. This equation also is dependent on both thickness of the anode catalyst region and the current density. So we varied the values of the thickness from 0.215 cm to 0.218 cm and current density from 0.05 to 0.15 A/cm^2 in equation (55) to get the methanol concentration at different current densities. The methanol concentration for different values of current densities is shown in the

Table 6.

Table 6

Methanol concentration for different current density in anode catalyst region (operating conditions temperature = 343K, pressure = 1 atm.)

Thickness (x) cm	Methanol concentration (M) for I_{cell} = 0.05 A/cm^2	Methanol concentration (M) for I_{cell} = 0.1 A/cm^2	Methanol concentration (M) for I_{cell} = 0.15 A/cm^2
0.215	3.11094E-04	3.02211E-04	2.93327E-04
0.216	3.11022E-04	3.02066E-04	2.9311E-04
0.218	3.10877E-04	3.01777E-04	2.9676E-04

In anode catalyst region also methanol concentration decreases with respect to the value of thickness (x) and this decreasing rate is minimum for low current density and maximum for higher current density. This is because of consumption of methanol in anode catalyst region during the methanol oxidation reaction methanol is consumed.

The methanol concentration in anode catalyst region is shown in the Fig. 10.

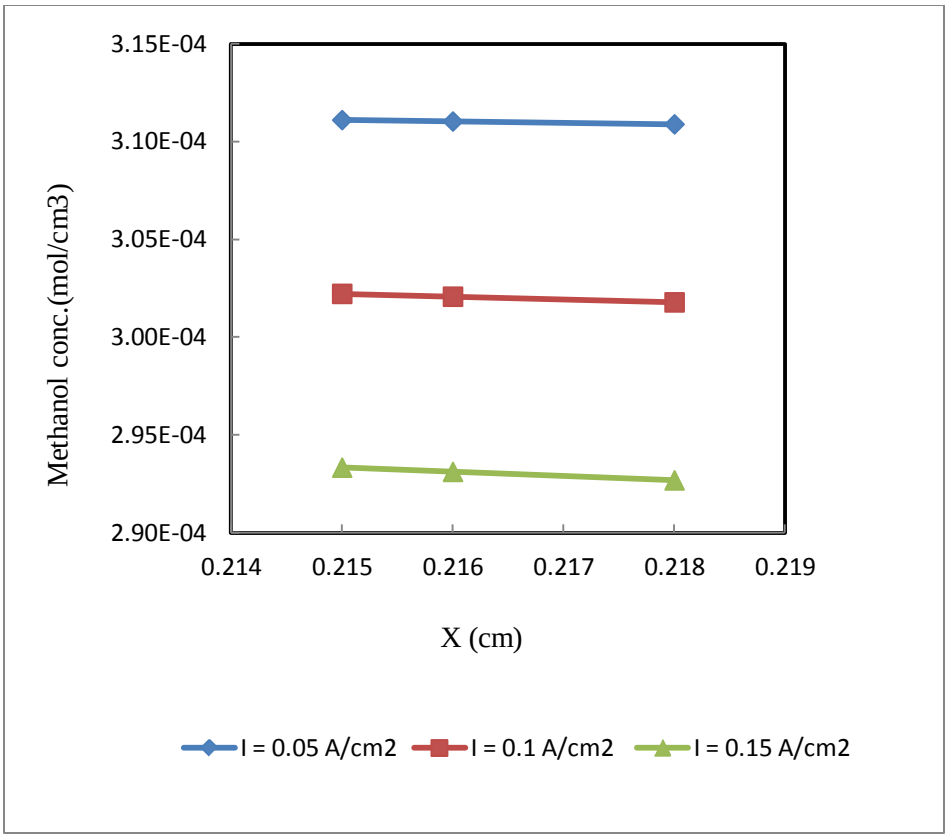

Fig. 10. Methanol concentration profiles in anode catalyst region (operating conditions: temperature = 343K, pressure = 1 atm.)

The model equations (53), (54) and (55) are solved using the parameters of Table 2. But when we use the Table 3 parameters we get the different equations for methanol concentration in anode flow and anode diffusion regions.

The solved model equation for methanol concentration in anode flow region using Table 2 parameters is (59). This equation also is independent of the thickness of the anode flow region and dependent to the current density only. So we varied the values of current density from 0.05 to 0.15 A/cm^2 in equation (59) to get the methanol concentration at different current densities. The methanol concentration for different values of current densities is shown in the Table 7.

Table 7

Methanol concentration for different current density in anode flow region (operating conditions temperature = 298K, pressure = 1 atm.)

Current density (A/cm^2)	Methanol concentration (M)
0.05	4.2811E-04
0.1	3.56E-04
0.15	2.8439E-04

As it has been discussed above that the methanol concentration in anode flow region is independent of the thickness (x) of the layer, therefore the graph of methanol concentration with respect to the thickness (x) will be constant as shown in the Fig. 11.

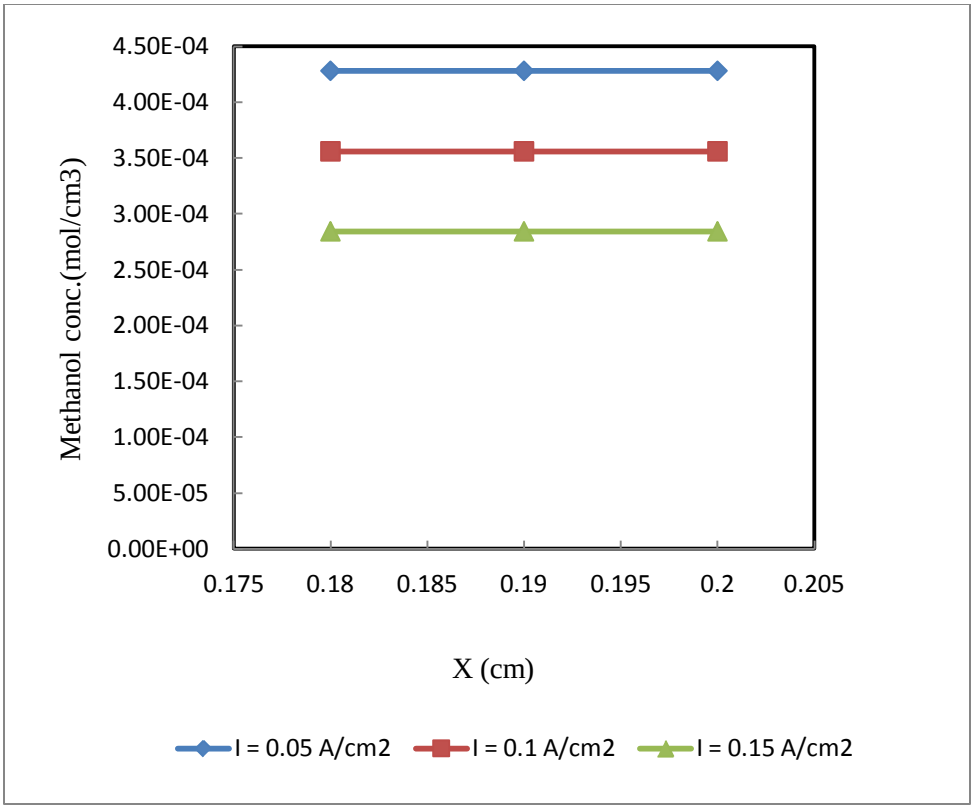

Fig. 11. Methanol concentration profiles in anode flow region (operating conditions: temperature 298K, pressure 1 atm.)

Methanol concentration is constant in the anode flow region because we have assumed that the anode flow region will be treated as a CSTR. For low current density methanol concentration is high while foe higher current density methanol concentration is lower.

Similarly model equations solved for methanol concentration in anode diffusion region using table 2 parameters is (60). This equation also is dependent on both thickness of the anode diffusion region and the current density. So we varied the values of the thickness from 0.2 cm to 0.21 cm and current density from 0.05 to 0.15 A/cm^2 in equation (60) to get the methanol concentration at different current densities. The methanol concentration for different values of current densities is shown in the following Table 8.

Table 8

Methanol concentration for different current density in anode diffusion region (operating conditions: temperature = 298K, pressure = 1 atm.)

Thickness (x) cm	Methanol concentration (M) for I_{cell} = 0.05 A/cm^2	Methanol concentration (M) for I_{cell} = 0.1 A/cm^2	Methanol concentration (M) for I_{cell} = 0.15 A/cm^2
0.2	3.42498E-04	2.85083E-04	2.27633E-04
0.205	2.80262E-04	1.60623E-04	4.09491E-05
0.21	2.18027E-04	3.61636E-05	

In anode diffusion region methanol concentration decreases with respect to the value of thickness (x) and this decreasing rate is minimum for low current density and maximum for higher current density. This is because diffusion takes place in the anode diffusion layer which decreases the methanol concentration.

The methanol concentration in anode diffusion region is shown in the Fig. 12.

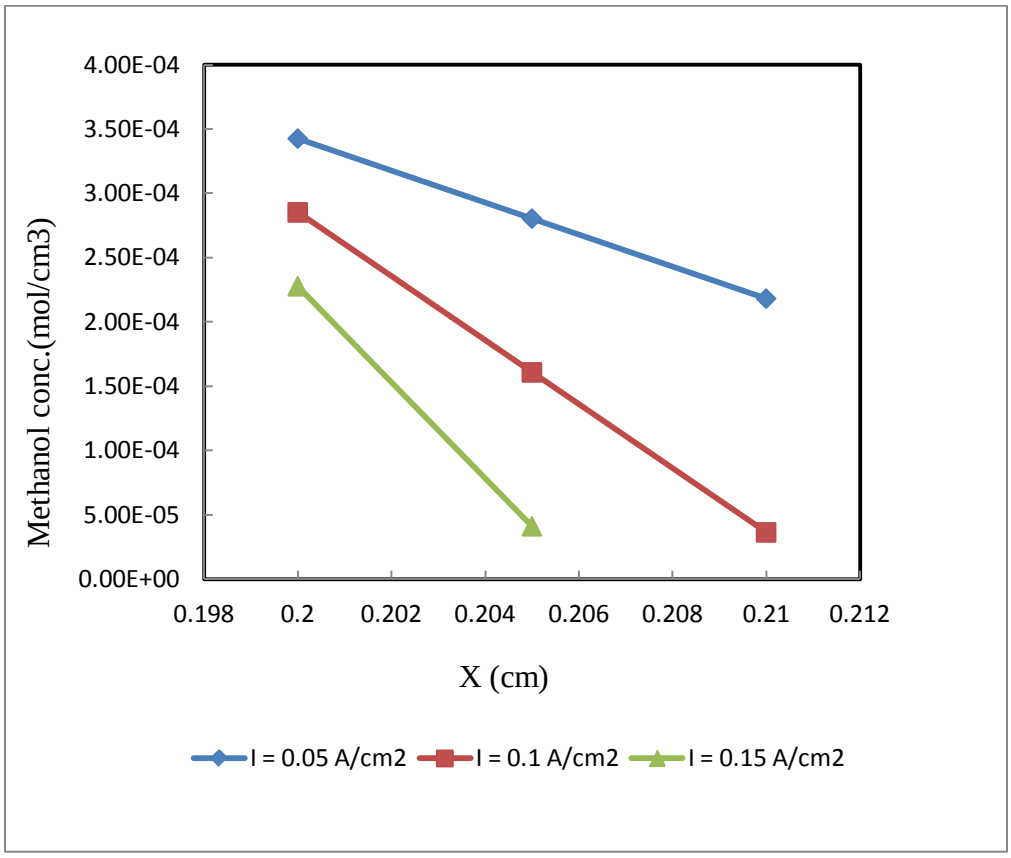

Fig. 12. Methanol concentration profiles in anode diffusion region (operating conditions: temperature = 298K, pressure = 1 atm.)

Oliveira *et al.* [58] also reported the similar results for methanol concentration profile in anode flow region. But in diffusion and catalyst regions authors reported the methanol concentration decreasing at a faster rate than the Fig. 9. and Fig. 10. This may be because of the different values of some parameters we are using like electro-osmotic drag coefficient of methanol (ξ_{CH_3OH}). The value of this parameter we are using is 7.5 [32]

But when we use the value of electro-osmotic drag coefficient of methanol (ξ_{CH_3OH}) as 1.99 (reference value) and Table 3 parameters the results for methanol concentration in anode flow and in anode diffusion are shown in the Fig. 11. and Fig. 12. respectively.

In the Fig. 11. and Fig. 12. also the nature of profile of methanol concentration is similar to that of Fig. 8. and Fig. 9. but in the anode diffusion region rate of decreasing is more which is more similar to Oliveira *et al.* [58].

Model equations solved for behavior of net water transport coefficient (α) with respect to the current density is (63). This equation is derived for 0.5M methanol concentration. This equation is dependent on current density. So we varied the value of current density from .05 to 0.15 A/cm^2 in equation (63) to get the behavior of net water transport coefficient (α). The net water transport coefficient (α) for different values of current densities is shown in the Table 9.

Table 9

Net water transport coefficient (α) for different values of current densities (operating conditions: temperature = 343K, pressure = 1 atm.)

Current density (A/cm^2)	Net water transport coefficient (α)
0.05	6.3804
0.1	4.68875
0.15	4.1177

Behavior of net water transport coefficient (α) with respect to the current density is shown in the Fig. 13. Here the net water transport coefficient is inversely proportional to the current density. In starting the net water transport coefficient is decreasing at a faster rate bur after a certain value of current density it becomes almost constant.

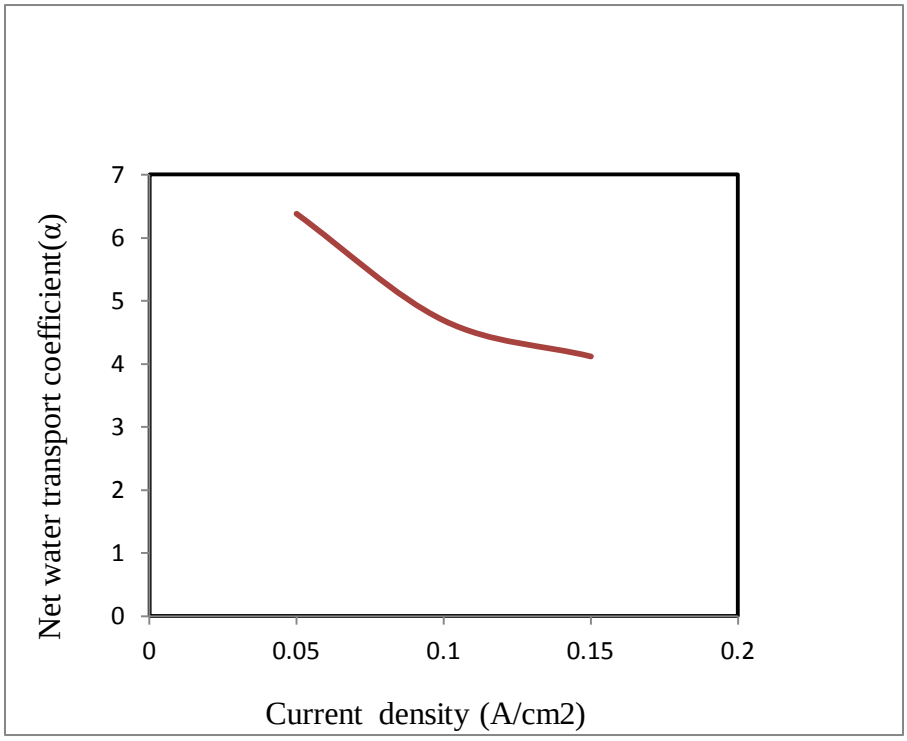

Fig. 13. Behavior of net water transport coefficient with respect to current density

Rangel *et al.*[59] also reported the similar curve for the behavior of net water transport coefficient with respect to the current density for 0.5M methanol concentration

Model equation (64) is solved for water concentration in anode flow region. This equation is independent of the thickness of the anode flow region and dependent to the current density only. So we varied the values of current density from 0.05 to 0.15 A/cm^2 in equation (64) to get the water concentration at different current densities. The water concentration for different values of current densities is shown in the Table 10.

Table 10

Water concentration for different current density in anode flow region (operating conditions: temperature = 343K, pressure = 1 atm.)

Current density (A/cm^2)	water concentration (M)
0.05	5.897386E-02
0.1	5.8947727E-02
0.15	5.8921591E-02

As it has been discussed above that the water concentration in anode flow region is independent of the thickness (x) of the layer, therefore the graph of water concentration with respect to the thickness (x) will be constant as shown in the Fig. 14.

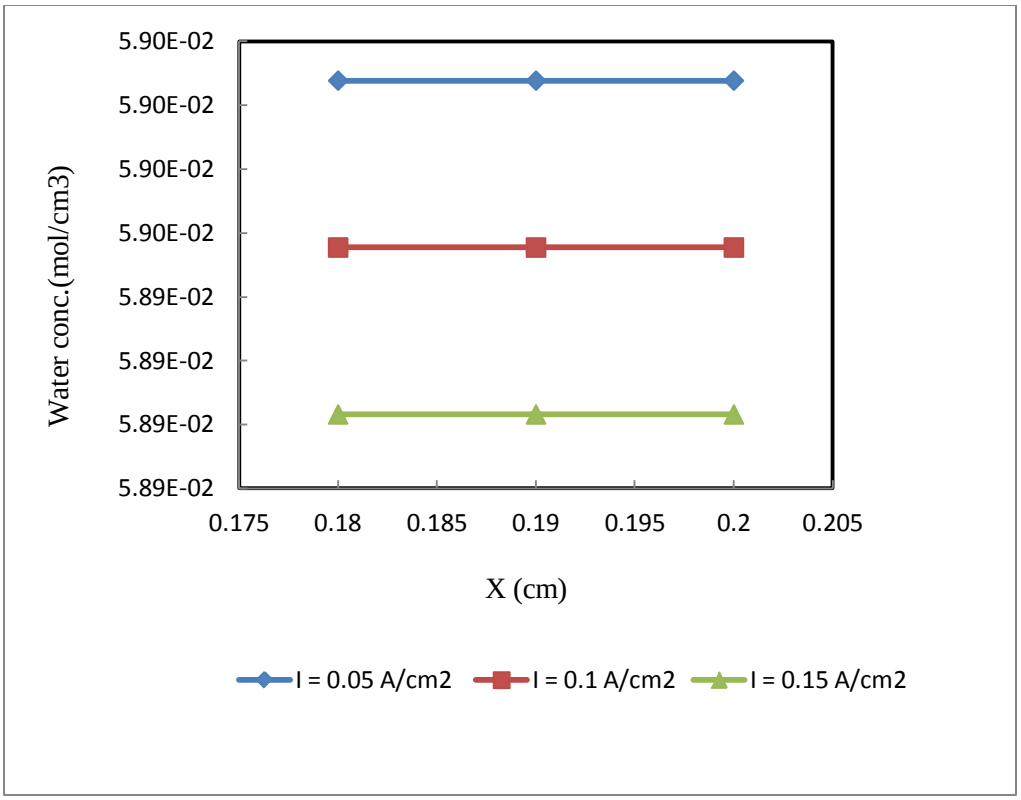

Fig. 14. Water concentration profiles in anode flow region (operating conditions: temperature = 343K, pressure = 1 atm.)

Water concentration is constant in the anode flow region because we have assumed that the anode flow region will be treated as a CSTR. For low current density water concentration is high while for higher current density water concentration is lower.

Similarly model equation (65) is solved for water concentration in anode diffusion region. This equation is dependent on both thickness of the anode diffusion region and the current density. So we varied the values of the thickness from 0.2 to 0.21 cm and current density from 0.05 to 0.15 A/cm^2 in equation (65) to get the water concentration at different current densities. The water concentration for different values of current densities is shown in the following Table 11.

Table 11

Water concentration for different current density in anode diffusion region (operating conditions temperature = 343K, pressure = 1 atm.)

Thickness (x) in cm	water concentration (M) for I_{cell} = 0.05 A/cm^2	water concentration (M) for I_{cell} = 0.1 A/cm^2	water concentration (M) for I_{cell} = 0.15 A/cm^2
0.2	4.71791E-02	4.715818E-02	4.713727E-02
0.205	4.717876E-02	4.71577E-02	4.71366E-02
0.21	4.717842E-02	4.715714E-02	4.713586E-02

Though the water diffusion takes place in AD and water consumption occur in AC, the concentration profile across these layers seems to be nearly constant. This can be understood by the fact that these layers are full of water, so the loss of water by diffusion and consumption is irrelevant when compared with the total amount of water present.

The water concentration in anode diffusion region is shown in the Fig. 15.

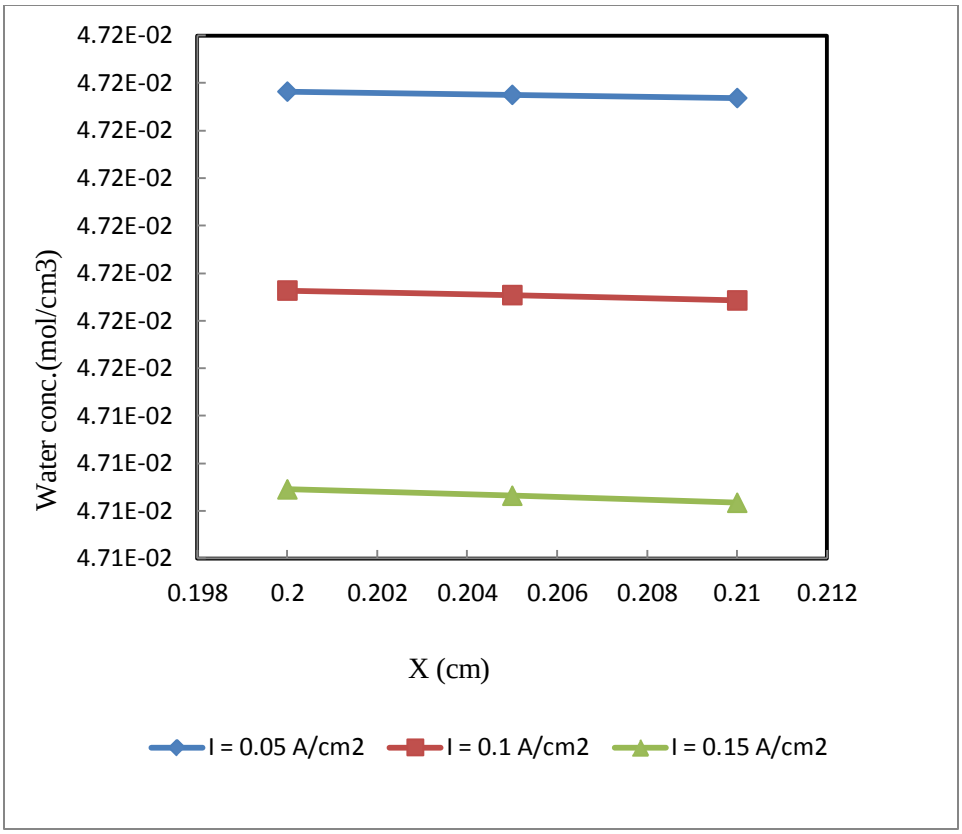

Fig. 15. Water concentration profiles in anode diffusion region (operating conditions: temperature = 343K, pressure = 1 atm.)

Similarly model equation (66) is solved for water concentration in anode catalyst region. This equation also is dependent on both thickness of the anode diffusion region and the current density. So we varied the values of the thickness from 0.2 to 0.21 cm and current density from 0.05 to 0.15 A/cm^2 in equation (66) to get the water concentration at different current densities. The water concentration for different values of current densities is shown in the following Table 12.

Table 12

Water concentration for different current density in anode diffusion region (operating conditions temperature = 343K, pressure = 1 atm.)

Thickness (x) cm	water concentration (M) for I_{cell} = 0.05 A/cm^2	water concentration (M) for I_{cell} = 0.1 A/cm^2	water concentration (M) for I_{cell} = 0.15 A/cm^2
0.2	3.77425E-02	3.7725298E-02	3.7708113E-02
0.205	3.774233E-02	3.7725075E-02	3.770783E-02
0.21	3.774203E-02	3.772463E-02	3.7707228E-02

The water concentration in anode catalyst region is shown in the Fig. 16.

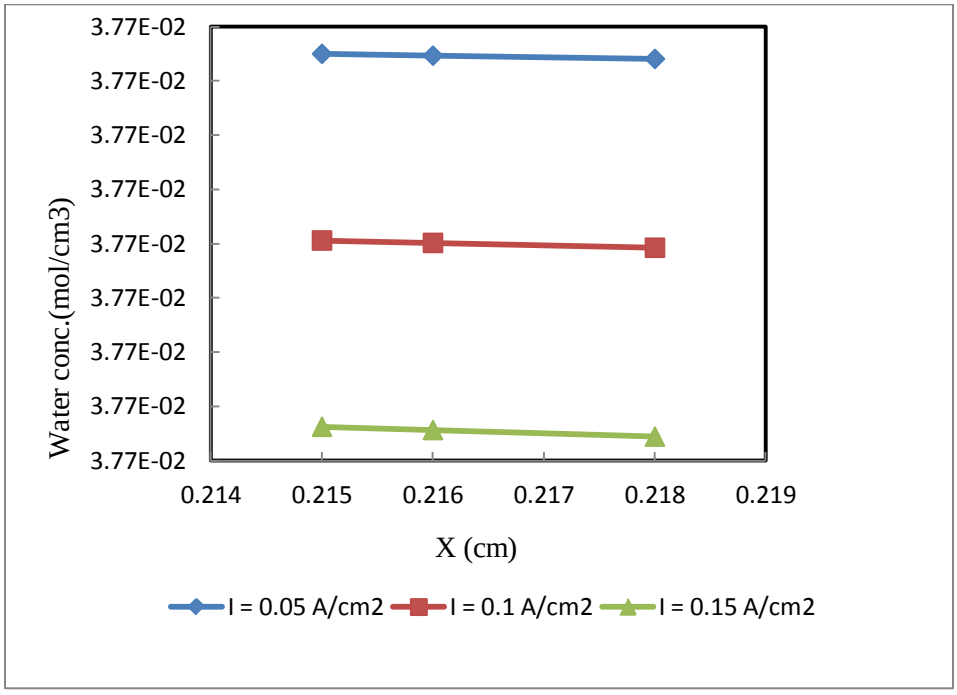

Fig. 16. Water concentration profiles in anode catalyst region (operating conditions: temperature = 343K, pressure = 1 atm.)

Conclusion

The model allows the determination of the effect of the operating parameters (such as oxygen and methanol feed concentrations, current densities of the direct methanol fuel cell) and the design parameters (such as active area, geometry, material properties) on the concentration profiles. An attention is given to the effects of various parameters such as current density and the methanol feed concentration on the water balance between cathode and anode in the direct methanol fuel cell (DMFC). In anode flow region the methanol concentration decreases with increasing current density of the direct methanol fuel cell and remains constant with respect to the thickness of the anode flow region. In anode diffusion layer the methanol concentration decreases with both current density of the direct methanol fuel cell and with the thickness of the anode diffusion layer. The decreasing rate of the methanol concentration in the anode diffusion region is more for higher current density and is less for lower current density of the direct methanol fuel cell. Similarly in anode catalyst layer the methanol concentration decreases with both current density of the direct methanol fuel cell and with the thickness of the anode catalyst layer. The model presented in thesis work can be a useful tool to enhance the direct methanol fuel cell understanding and for the optimization of fuel cell design.

References

1. A.S. Arico, S. Srinivasan and V. Antonucci “DMFCs: From Fundamental Aspects to Technology Development” FUEL CELLS 2001, 1, No.2

2. Anna Monis Shipley and R. Neal Elliott “Stationary Fuel Cells: Future Promise, Current Hype” American Council for a Energy-Efficient Economy, 2004, Report No. IE041

3. R. Dillon , S. Srinivasan , A. S. Aricò and V. Antonucci “International activities in DMFC R&D: status of technologies and potential applications” Journal of Power Sources, Volume 127, Issues 1-2, 10 March 2004, Pages 112-126

4. Michel Broussely and Graham Archdale “Li-ion batteries and portable power source prospects for the next 5–10 years“ Journal of Power Sources, Volume 136, Issue 2, 1 October 2004, Pages 386-394

5. Gogel , T. Frey , Zhu Yongsheng , K. A. Friedrich , L. Jörissen and J. Garche “Performance and methanol permeation of direct methanol fuel cells: dependence on operating conditions and on electrode structure” Journal of Power Sources, Volume 127, Issues 1-2, 10 March 2004, Pages 172-180

6. G. Q. Lu and C. Y. Wang “Electrochemical and flow characterization of a direct methanol fuel cell” Journal of Power Sources, Volume 134, Issue 1, 12 July 2004, Pages 33-40

7. Lindermeir , G. Rosenthal , U. Kunz and U. Hoffmann “On the question of MEA preparation for DMFCs” Journal of Power Sources, Volume 129, Issue 2, 22 April 2004, Pages 180-187

8. Harry Hoster, Teresa Iwasita, Hermann Baumgärtner and Wolf Vielstich “Pt-Ru model catalysts for anodic methanol oxidation: Influence of structure and composition on the reactivity” Phys. Chem. Chem. Phys., 2001, 3, 337-346

9. Zhaobin Wei, Suli Wang, Baolian Yi, Jianguo Liu, Likang Chen, WeiJiang Zhou, Wenzheng Li and Qin Xin “Influence of electrode structure on the performance of a direct methanol fuel cell” Journal of Power Sources, Volume 106, Issues 1-2, 1 April 2002, Pages 364-369

10. H. Yang and T.S. Zhao “Effect of anode flow field design on the performance of liquid feeddirect methanol fuel cells“ Electrochimica Acta, In Press, Corrected Proof, Available online 12 January 2005,

11. K. Sundmacher, T. Schultz, S. Zhou, K. Scott, M. Ginkel and E. D. Gilles “Dynamics of the direct methanol fuel cell (DMFC): experiments and model-based analysis” Chemical Engineering Science, Volume 56, Issue 2, January 2001, Pages 333-341

12. Lindermeir, G. Rosenthal , U. Kunz and U. Hoffmann “On the question of MEA preparation for DMFCs” Journal of Power Sources, Volume 129, Issue 2, 22 April 2004, Pages 180-187

13. G. Q. Lu and C. Y. Wang “Electrochemical and flow characterization of a direct methanol fuel cell” Journal of Power Sources, Volume 134, Issue 1, 12 July 2004, Pages 33-40

14. Gaby J.M. Janssan, Michel P. de Heer, Dimitrios C. Papageorgopoulos “Development of Bilayer Anodes for Improved reformate Tolerance of PEM Fuel Cells” Energy research Centre of the Netherlands ECN, Fuel CellTechnology, P.O. Box1, 1755 ZG Petten / The Netherlands

15. Gogel , T. Frey , Zhu Yongsheng , K. A. Friedrich , L. Jörissen and J. Garche “Performance and methanol permeation of direct methanol fuel cells: dependence on operating conditions and on electrode structure” Journal of Power Sources, Volume 127, Issues 1-2, 10 March 2004, Pages 172-180

16. Nordlund, J.; Roessler, A.; Lindbergh, G. “The influence of electrode morphology on the performance of a DMFC anode” Journal of Applied Electrochemistry, Volume 32, Issue 3, 2002 March, Pages 259- 265

17. Sylvie Escribano and Pierre Aldebert “Electrodes for hydrogen/oxygen polymer electrolyte membrane fuel cells” Solid State Ionics, Volume 77, April 1995, Pages 318-323

18. S. Hikita, K. Yamane and Y. Nakajima, Measurement of methanol crossover in direct methanol fuel cell, JSAE Review 22 (2001) 151-156.

19. S. P. Nunes, B. Ruffmann, E. Rikowski, S. Vetter and K. Richau ”Inorganic modification of proton conductive polymer membranes for direct methanol fuel cells”Journal of Membrane Science, Volume 203, Issues 1-2, 30 June 2002, Pages 215- 225

20. Weilin Xu, Tianhong Lu, Changpeng Liu and Wei Xing “Low methanol permeable composite Nafion/silica/PWA membranes for low temperature direct methanol fuel cells”

21. Youngcho Si, Jung-chou Lin, H. Russel Kunz and James M. Fenton “Trilayer membranes with a Methanol-Barrier Layer for DMFCs” Journal of the Electrochemical Society, 151 (3) A463-A469 (2004)

22. Ilie Fishtik, Caitlin A. Callaghan, and Ravindra Datta “Reaction Route Graphs. I. Theory and Algorithm” J. Phys. Chem. B 2004, 108, 5671-5682

23. Ilie Fishtik, Caitlin A. Callaghan, and Ravindra Datta “Reaction Route Graphs. II. Examples of Enzyme- and surface-Catalyzed Single Overall Reactions” J. Phys. Chem. B 2004, 108, 5683-5697

24. H. Dohle, J. Divisek, J. Mergel, H.F. Oetjen, C. Zingler and D. Stolten, Recent developments of the measurement of the methanol permeation in a direct methanol fuel cell, Journal of Power Sources 105 (2002) 274-282.

25. Harrell Sellers and Evgeny Shustorovich “Intrinsic activation barriers and coadsorption effects for reactions on metal surfaces: unified formalism within the UBI-QEP approach“ Surface Science, 504, 2002, 167-182

26. Amit A. Gokhale, Shampa Kandoi, Jeffrey P. Greeley, Manos Mavrikakis and James Dumesic “Molecular-level descriptions of surface chemistry in kinetic models using density functional theory” Chemical Engineering Science, Volume 59, Issues 22-23, November-December 2004, Pages 4679-4691

27. Snezana Lj. Gojković “Mass transfer effect in electrochemical oxidation of methanol at platinum electrocatalysts” Journal of Electroanalytical Chemistry, Volume 573, Issue 2, 1 December 2004, Pages 271-276

28. A.J. Appleby, F.R. Foulkes “Fuel Cell Handbook (Sixth Edition)” CRC Press, ISBN: 0849308771 August, 2002

29. Alfred B. Anderson “Theory at the electrochemical interface: reversible potentials and potentialdependent activation energies” Electrochimica Acta, Volume 48, Issues 25-26, 15 November 2003, Pages 3743-374

30. B. L. García, V. A. Sethuraman, J. W. Weidner, R. E. White, Mathematical Model of a Direct Methanol Fuel Cell, Journal of Fuel Cell Science and Technology Vol.1, November 2004, 43-48.

31. Reid RC, Prausnitz JM, Sherwood TK. The properties of gases and liquids. New York: McGraw-Hill; 1977

32. Determination of Electroosmotic Drag Coefficients for Water and Methanol in Membranes for DMFC T. Tschinder, B. Evers, T. Schaffer, V. Hacker, J.O. Besenhard,

33. M. Watanabe, S. Saegusa and P. Stonehart, High platinum electrocatalyst utilizations for direct methanol oxidation, Journal of Electroanalytical Chemistry 271 (1989) 213-220.

34. R. Parsons and T. Vandernoot, The oxidation of small organic molecules: A survey of recent fuel cell related research, Journal of Electroanalytical Chemistry 257 (1988) 9-45.

35. K. Ramya, K.S. Dhathathreyan, Direct methanol fuel cells: determination of fuel crossover in a polymer electrolyte membrane, Journal of Electroanalytical Chemistry 542 (2003) 109-115.

36. M. P. Hogarth and G. A. Hards, Direct Methanol Fuel Cells: Technological advances and further requirements, Platinum Metals Review 40 (1996) 150-159.

37. N. Munichandraiah, K. McGrath, G. Prakash, R. Aniszfeld and G. Olah, A potentiometric method of monitoring methanol crossover through polymer electrolyte membranes of direct methanol fuel cells, Journal of Power Sources 117 (2003) 98-101.

38. K. Chandrasekaran, J. C. Wass, and J. O' M. Bockris, The Potential Dependence of Intermediates in Methanol Oxidation Observed in the Steady State by FTIR Spectroscopy, Journal of the Electrochemical Society 137 (1990) 518-524.

39. J.Y. Park, J.H. Lee, S. Kang, J. Sauk and I. Song, Mass balance research for high electrochemical performance direct methanol fuel cells with reduced methanol crossover at various operating conditions, Journal of Power Sources 178 (2008) 181-187.

40. Y. Morimoto and E. B. Yeager, Comparison of methanol oxidations on Pt, Pt/Ru and PtSn electrodes, Journal of Electroanalytical Chemistry 444 (1998) 95-100.

41. A. B. Anderson, E. Grantscharova and S. Seong, Systematic Theoretical Study of Alloys of Platinum for Enhanced Methanol Fuel Cell Performance, Journal of the Electrochemical Society 143 (1996) 2075-2082.

42. V. Gogel, T. Frey, Z. Yongsheng, K.A. Friedrich, L. Jörissen and J. Garche, Performance and methanol permeation of direct methanol fuel cells: dependence on operating conditions and on electrode structure, Journal of Power Sources 127 (2004) 172-180.

43. K.L. Ley, R. Liu, C. Pu, Q. Fan, N. Leyarovska, C. Segre and E.S. Smotkin, Methanol Oxidation on Single-Phase Pt/Ru-Os Ternary Alloys, Journal of the Electrochemical Society 144 (1997) 1543-1548.

44. L. Liu, R. Viswanathan, R. Liu and E.S. Smotkin, Methanol Oxidation on Nafion Spin-Coated Polycrystalline Platinum and Platinum Alloys, Electrochemical and Solid State Letters 1 (1998) 123-125.

45. C. Pu, W. Huang, K.L. Ley and E.S. Smotkin, A methanol impermeable proton conducting composite electrolyte system, Journal of the Electrochemical Society 142 (1995) L119-L120.

46. J.S. Wainright, J.-T. Wang, D. Weng, R.F. Savinell and M. Litt, Acid-Doped Polybenzimidazoles: A new polymer electrolyte, Journal of the Electrochemical Society 142 (1995) L121-L123.

47. J.T. Wang, J.S. Wainright, R.F. Savinell and M. Litt, A direct methanol fuel cell using acid-doped polybenzimidazole as polymer electrolyte, Journal of Applied Electrochemistry 26 (1996) 751-756.

48. A. Küver and K. Potje-Kamloth, Comparative study of methanol crossover across electropolymerized and commercial proton exchange membrane electrolytes for the acid direct methanol fuel cell, Electrochimica Acta 43 (1998) 2527-2535.

49. V. Tricoli, Proton and methanol transport in poly(perfluorosulfonate) membranes containing Cs^+ and H^+ cations, Journal of the Electrochemical Society 145 (1998) 3798-3801.

50. W. C. Choi, J. D. Kim and S. I. Woo, Modification of proton conducting membrane for reducing methanol crossover in a direct-methanol fuel cell, Journal of Power Sources 96 (2001) 411-414.

51. L.J. Hobson, Y. Nakano, H. Ozu and S. Hayase, Targeting improved DMFC performance, Journal of Power Sources 104 (2002) 79-84.

52. H. Uchida, Y. Mizuno and M. Watanabe, Suppression of methanol crossover and distribution of ohmic resistance in Pt- dispersed PEMs under DMFC operation,

53. Journal of the Electrochemical Society 149 (2002) A682-A687.

54. N.A. Hampson, M.J. Willars and B.D. McNicol, The methanol-air fuel cell: A selective review of methanol oxidation mechanisms at platinum electrodes in acid electrolytes, Journal of Power Sources 4 (1979) 191-201.

55. C.Y. Du, T.S. Zhao and W.W. Yang, Effect of methanol crossover on the cathode behaviour of a DMFC: A half-cell investigation, Electrochimica Acta 52 (2007) 5266–5271.

56. R. Jiang and D. Chu, Comparative studies of methanol crossover and cell performance for a DMFC, Journal of the Electrochemical Society 151 (2004) 69- 76.

57. K. Scott, W. Taama, J. Cruickshank, J. Power Sources 65 (1997) 159.

58. Oliveira, V.B, Falcão, D.S., Rangel, C.M. and Pinto, A.M.F.R., Heat and mass transfer effects in a direct methanol fuel cell: A 1D model, International Journal of Hydrogen Energy, Vol. 33, Issue 17, July 2008 3818-3828.

59. Oliveira, V.B, Rangel, C.M. and Pinto, A.M.F.R., Water management in direct Methanol Fuel Cells, International Journal of Hydrogen Energy (2009), doi:10.1016/j.ijhydene.2009.07.111

60. https://en.wikipedia.org/wiki/Direct methanol fuel cell

.

.